Available online at www.sciencedirect.com
SCIENCE DIRECT
Polymer 46 (2005) 10355–10363
polymer
www.elsevier.com/locate/polymer

Orientation of multiwalled carbon nanotubes in composites with polycarbonate by melt spinning

Petra Pötschke*, Harald Brünig, Andreas Janke, Dieter Fischer, Dieter Jehnichen

Leibniz Institute of Polymer Research Dresden, Hohe Str. 6, D-01069 Dresden, Germany

Received 22 April 2005; received in revised form 18 July 2005; accepted 29 July 2005
Available online 24 August 2005

Abstract

A conductive polycarbonate (PC) composite containing 2 wt% multiwalled carbon nanotubes (MWNT) and pure PC were melt spun using a piston type spinning device. Different take-up velocities up to 800 m/min and throughputs leading to draw down ratios up to 250 were used. The composite material of PC with MWNT was prepared by diluting a PC based masterbatch consisting of 15 wt% MWNT by melt mixing in an extruder. The alignment of the nanotubes within melt spun fibers with draw down ratios up to 126 was investigated by TEM and Raman spectroscopy. The nanotubes align in their length axis along the fiber axis increasingly with the draw down ratio, however, the curved shape of the nanotubes still exist in the melt spun fibers. At higher draw down ratios, the MWNT started to align by reducing their curvature. Polarized Raman spectroscopy indicated that the *D*/*D* and *G*/*G* ratios parallel/perpendicular to the fiber axis increase for both MWNT bands in a similar manner with the draw down ratio. Interestingly, with increasing alignment electrical conductivity of the fibers is lost. Mechanical investigations revealed that at low spinning speeds elongation at break and tensile strength of the composite are lower than those of the pure PC. However, at the highest take-up velocity of 800 m/min the elongation at break is higher and true stress at break of the composite fiber is comparable to the pure PC fiber.

Keywords: Multiwalled carbon nanotube composites; Polycarbonate; Melt spinning

1. Introduction

The global market for chemical fibers and yarns is steadily increasing with growing world population [1]. With that the demand for new industrial fibers with special or improved properties emerges. Among other things, stronger and/or electrical conductive fibers are requested for applications as reinforcement fibers, smart clothing, electromagnetic shields or armors, for instance [2,3]. Addition of fillers is widely applied to make polymers electrically conductive and to improve their mechanical properties. For production of fibers with diameters ranging between 10 and 100 μm, however, only nanoscaled fillers can be used. The superior association of their inherent good mechanical and electrical properties makes carbon nanotubes exceptionally interesting for the production of such fibers. Indeed the prices for nanotubes are still much too high for commercial success, however, the prices are falling continually and a breakthrough is expected within the next years. By then it is important to develop suitable techniques for industrial fiber fabrication.

One of the most important and challenging tasks is the incorporation of the nanotubes into a polymeric matrix in order to transfer their excellent properties to the macroscopic material scale. For this purpose singlewalled carbon nanotubes (SWNT) seem to be more preferable as compared to multiwalled carbon nanotubes (MWNT) because of the smaller diameter and therefore, higher aspect ratio, the higher mechanical properties, and the possible higher load transfer because of easier bonding opportunities to polymer chains. In MWNT also a sliding or telescopic mechanism is discussed under mechanical stress. For both materials, uniform distribution and dispersion is indispensable in order to transfer the excellent properties into a polymeric matrix. Kumar et al. [4] used in situ polymerization of poly-(*p*-phenylene benzobisoxazole) in the presence of SWNT which were brought into a stable dispersion. By means of a dry-jet wet spinning process the products were spun to

* Corresponding author. Tel.: +49 351 4658395; fax: +49 351 4658565.
E-mail address: poe@ipfdd.de (P. Pötschke).

0032-3861/$ - see front matter © 2005 Elsevier Ltd. All rights reserved.
doi:10.1016/j.polymer.2005.07.106

fibers, which exhibited a 60% increased tensile strength as compared to reference material. Kearns and Shambaugh [5] used a solvent process to disperse SWNT in polypropylene (PP). After removing the solvent, fibers were melt spun which exhibited an increased tensile strength up to 40%. Haggenmueller et al. [6] used a combination of solvent casting and melt mixing for producing poly (methyl methacrylate) (PMMA)/SWNT composite fibers. Thereby, the melt mixing step was shown to enhance the nanotubes dispersion. For a broad technical application melt mixing with subsequently melt spinning is mostly interesting. Siochi et al. [7] successfully incorporated SWNT into polyimide using melt processing whereas Haggenmueller et al. [8] showed examples for melt spun fibers prepared from melt mixed polystyrene (PS)/SWNT and polyethylene (PE)/MWNT composites. Bhattacharyya et al. [9] melt mixed and melt spun PP/SWNT fibers with a melt filtering procedure to remove larger SWNT agglomerates.

Only a few examples [10,11] are shown for fibers made by incorporation of MWNT into polymer matrices following this route. However, in these examples fiber forming was performed more or less by drawing an extrudate and thus, only low degrees of alignment could be achieved. No systematic investigations are known about the influencing of draw down ratio achieved by melt spinning on alignment of nanotubes and mechanical properties of their composites.

From conventional fiber reinforcement it is well known that unidirectional composites show the highest improvements in strength and modulus. Therefore, it is expected that alignment of nanotubes is important for improved mechanical properties. Especially, the production of fibers makes it possible to get a controlled orientation and/or alignment of the nanoscaled fillers in macroscopic part. Alignment is understood as a preferred orientation of a tube (or its longitudinal axes) within a three-dimensional sample, which can be accompanied by disentanglement or stretching of curved tubes. Siochi et al. [7] investigated SWNT/polyimide composites and characterized the SWNT orientation characterized more or less roughly by comparison of Raman spectra parallel and perpendicular to the fiber axis and high resolution scanning electron microscopy (HRSEM) on solvent treated cross sections. The authors found an increased yield stress for the fibers with aligned SWNT respective to unoriented films. Sennet et al. [10] used transmission electron microscopy (TEM) to visualize the orientation of MWNT and SWNT in polycarbonate (PC) based fibers and found regardless of the molecular weight of the PC used an increasing orientation of MWNT with draw speeds varied up to 70 m/min. Haggenmueller et al. applied polarized Raman spectroscopy on PMMA/SWNT [6] and PE/SWNT [8] fibers and used the Raman intensity of the radial breathing mode at 202 cm^{-1} as function of the angle with respect to the incident polarization axis [6] or the intensity ratio parallel/perpendicular [8] to determine the full width at half maximum (FWHM) of the distribution function. The FWHM decreased indicating enhanced alignment with reducing the fiber diameter because of higher extensional flow and lower loadings because of higher freedom to flow and to align. Bhattacharyya et al. [9] determined the SWNT Herman's orientation factor of PP/SWNT composites from polarized Raman spectroscopy by using the peak intensity of the tangential mode at $\sim$1592 cm^{-1} at different angles between fiber axis and polarization direction. Sreekumar et al. [12] used the same procedure for polyacrylonitrile/SWNT composite fibers.

X-ray diffraction experiments are quite commonly used in order to characterize the degree of alignment for SWNT in macroscopic fibers. For this the azimuthal intensity distribution at the wave vector corresponding to characteristic peaks of SWNT and SWNT bundles are used as demonstrated in [13]. Next to the wide-angle region also the small-angle region can be used to determine the FHWM as shown by Zhou et al. [14] and Du et al. [15]. Du et al. found an increase in FWHM with SWNT loading in PMMA/PS melt spun fibers using the small-angle region which was consistent with the FWHM increase reported in [8]. Sandler et al. [11] used WAXS diffraction patterns to make an assessment for alignment of MWNT in melt processed polyamide 12 (PA12) composite fibers. However, the authors did not find changed azimuthal intensity distribution of the (002) reflection of the graphite layers in a strained fiber. It seems that polarized Raman spectroscopy and X-ray scattering methods are nicely applicable in order to quantify the state of nanotube alignment in composites containing SWNT. However, these methods could not be successfully applied to MWNT based composite fibers.

2. Experimental

2.1. Materials and melt spinning

The composite of polycarbonate (PC) with 2 wt% of multiwalled carbon nanotubes (PC-2NT) was produced by diluting a masterbatch of 15 wt% multiwalled carbon nanotube in polycarbonate, supplied by Hyperion Catalysis International, Inc. (Cambridge, MA, USA), with pure PC (Iupilon E-2000, Mitsubishi Engineering Plastics) using a Haake co-rotating, intermeshing twin-screw extruder ($D=30$, $L/D=10$) as previously described [16]. Before processing PC was dried for at least 4 h at 120 °C under vacuum atmosphere.

Melt rheological properties of unmodified PC and PC with 2 wt% MWNT were obtained using an ARES oscillatory rheometer (Rheometric Scientific) at 260 °C in nitrogen atmosphere using a parallel plate geometry (plates 25 mm diameter, gap of 1–2 mm). Granules were placed between the preheated plates and allowed to equilibrate for about 3 min. Frequency sweeps were performed between 0.1 and 100 rad/s (for PC) and 0.025 and 100 rad/s (for PC-2NT) at strains within the linear viscoelastic range.

Table 1
Melt spinning conditions and sample designation

Run no.	Material	Throughput (cm^3/min)	Take-up velocity (m/min)	Draw down ratio (−)
	PC E-2000			
A2		0.45	50	7.8
A3		0.45	200	31.4
A4		0.45	800	126.0
A5		0.225	50	15.7
A6		0.225	200	62.8
A7		0.225	800	251.0
	PC E-2000 +2% MWNT			
B1		0.45	50	7.8
B2		0.45	200	31.4
B3		0.45	400	62.8
B4		0.45	800	126.0
B5		0.225	50	15.7
B6		0.225	200	62.8
B7		0.225	400	126
B8		0.225	800	251.0

Repeated sweeps with increasing and decreasing frequency were performed in order to check the stability of the sample over time (each sweep requires approximately 8 min) and the second sweep was interpreted.

Melt spinning was performed for as supplied PC Iupilon E-2000 granules and the PC based composite with 2 wt% MWNT. The melt spinning experiments were carried out by means of a self-constructed piston type spinning device. The upper part of the device consists of a drive train and a heatable cylinder with piston, closed by a single hole die (Fig. 1). The diameter of the capillary die hole was 0.3 mm, its length 0.6 mm. The adjustable speed of the piston determines the mass throughput of the molten polymer. A moveable winder is fixed below the die at a distance of 1 m to the die exit for collecting the extruded fiber. The winder allows to change the take-up velocity of the fiber within the range of 50 until 1400 m/min leading to different draw down ratios (ddr) of the fibers. In addition, a sample without using the winder was collected (named 'as extruded').

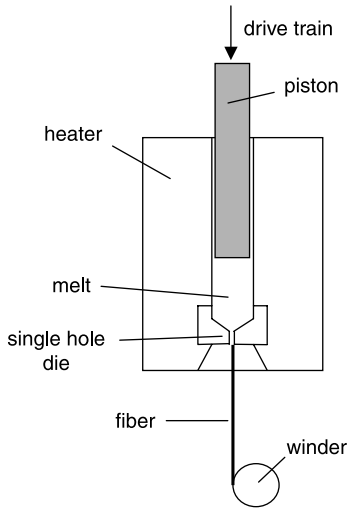

Fig. 1. Schema of the piston type spinning device.

For each run the dried material (up to 10 g) was filled under nitrogen into the cylinder and then it was heated up to the spinning temperature to get the molten state. After 10 min the extrusion was started. The spinning temperature for all runs was 280 °C. The driving force of the piston was measured and the melt pressure within the die was estimated taking into account the cross-section of the piston. The melt spinning conditions are summarized in Tables 1 and 2.

Estimation of the maximum shear rate within the die leads to values of about 3000 s^{-1}, the maximum elongation rate in the fiber building zone about 50–150 s^{-1} at 50 and 800 m/min take-up velocity, respectively. Even if the shear rates in the die are higher than the elongational rates, the elongational flow is responsible for the orientation of the polymer chains and carbon nanotubes within the fibers after leaving the die and acts over about 5–10 cm fiber length before solidification is finished.

2.2. Transmission electron microscopy

For transmission electron microscopy (TEM), the fibers were imbedded into an epoxy material (Epofix). The cuts were made along the fiber axis using a Reichert Ultracut S ultramicrotom (Leica, Austria) equipped with a diamond knife with a cut angle of 35° (Diatome, Switzerland) at room temperature. An angle between fiber axis and cut axis of 35° was chosen in order to ensure no alignment induced by the cutting procedure. A relatively high thickness of 200 nm of the thin sections was chosen in order to get a good balance between a high amount of structure elements in the section and a suitable sample transparency. The TEM used is an EM 912 (Zeiss, Germany) operated at 120 kV and the micrographs were taken in defocusing contrast in order to visualize the nanotubes.

Table 2
Results of spinning experiments, throughput 0.45 cm^3/min, 280 °C

Run no.	Material	v (m/min)	ddr (−)	p (bar)	D (μm)	Tt (dtex)	ε_B (%)	σ_B (cN/dtex)	σ_B (MPa)
	PC E-2000								
A2		50	7.8	118	95	84	223	4.3	516
A3		200	31.4	118	50	21	157	4.5	540
A4		800	126	118	23.4	5.2	51	4.1	492
	PC E-2000+2% MWNT								
B1		50	7.8	78	93.1	84	171	2.4	288
B2		200	31.4	78	50	21	148	3.0	360
B3		400	62.8	78	35	11	–	–	–
B4		800	126	78	24.5	5.2	72	3.9	468

v, take-up velocity; ddr, draw down ratio; p, melt pressure; Tt, fineness; ε_B, elongation at break; σ_B, (true) break stress.

2.3. Raman spectroscopy

The spectra were collected on two different Raman microscopes. First one was a Nikon microscope (50× objective) on the BRUKER FT Raman Modul FRA 106 (connected with the BRUKER FTIR spectrometer EQUINOX 55), equipped with a Ge-detector, with an excitation laser at 1064 nm, with both the incident and the 180° backscattered light parallel to the fiber axis. The laser power was 2 mW on the sample, the laser spot 2 μm and the resolution 4 cm^{-1}. The spectra were fitted by the Levenberg-Marquardt algorithm (BRUKER OPUS software) in the range from 2000 to 200 cm^{-1}. Second one was BH2-Olympus microscope (50× objective) on a DILOR XY Raman spectrometer, equipped with a LN_2 cooled CCD camera, with an excitation laser at 514.5 nm. The laser power was 1 mW, the laser spot 2 μm and the resolution 1 cm^{-1}. For polarized Raman spectra the fiber was rotated 90°, so that the direction of the *E*-vector of the polarized laser light was parallel and perpendicular oriented to the fiber axis. All spectra were baseline corrected and peak position and intensity were fitted by the Levenberg-Marquardt algorithm (DILOR software) in the range from 1100 to 1700 cm^{-1}.

2.4. Mechanical testing

The tensile properties of the fibers were determined by force-elongation experiments using a Goodbrand Universal Tester on single fibers. Five tests were performed for each sample using an initial sample length of 50 mm. A pretension of 0.05 cN/dtex was used. The test speed was adapted to the elongation at break (ε_b) and varied between 25 mm/min for the samples with $59\% < \varepsilon_b < 100\%$ and 200 m/min for samples with $200\% < \varepsilon_b < 400\%$. The fineness and diameter were measured by weighting and using an optical microscope, respectively. The Young's modulus was determined as the secant modulus at 1% strain. The measurements were done in an air-conditioned laboratory with 23 °C and 55% relative humidity. For conversion of fiber specific stress values a density value of 1.20 g/cm^3 was used for both, PC and PC with 2 wt% MWNT.

2.5. Electrical resistivity measurements

Electrical resistivity of the starting materials was measured using a Keithley 8009 Resistivity Test Fixture combined with a Keithley 6517A Electrometer on compression molded sheets (thickness 0.35 mm, diameter 70 mm) for the pure PC and using a 4-point method using a Keithley DMM 2000 Multimeter on strips (20×2 mm^2) cut from the sheets. For the melt spun fibers, bundles consisting of 50–400 fibers were tried to measure using an 8002A High Resistance Test Fixture for fibers and films.

2.6. Other investigations to assign the degree of alignment

According to common investigations in previous papers on fiber spinning we also tried to apply WAXS and SAXS method to the melt spun fibers which were investigated as fiber bundles. Because of the low content of MWNT in the samples combined with the curved structure of the nanotubes, the WAXS reflection assigned to the (002) peak of the hexagonal graphite structure (layer spacing within the MWNT) at ~26.5° (corresponding to 3.36 Å) appears as a clear peak in the two-dimensional WAXS pattern at high MWNT concentration, e.g. like in the masterbatch with 15 wt% MWNT. However, it not very clearly seen in the composites with 2 wt% MWNT and its melt spun fibers. Therefore, the azimuthal intensity distribution of this reflection as a measure of the alignment of the MWNTs was not possible to determine.

In the SAXS investigations performed the scattering behavior could not be attributed to the MWNT alignment solely. Here, it has to be considered the dominant contribution of the interfaces between the fibers and the surrounding medium within the fiber bundles to the scattered intensity. The interface scattering gives rise to so-called streaks within the equatorial region of the fiber diagram. With increasing take-up velocity the fiber diameter decreased thus leading to changed contributions of this scattering part. In order to prevent this phenomenon, Du et al. [15] performed SAXS investigations on a composite material prepared from wound up PMMA/SWNT fibers which were weld together and then hot pressed by

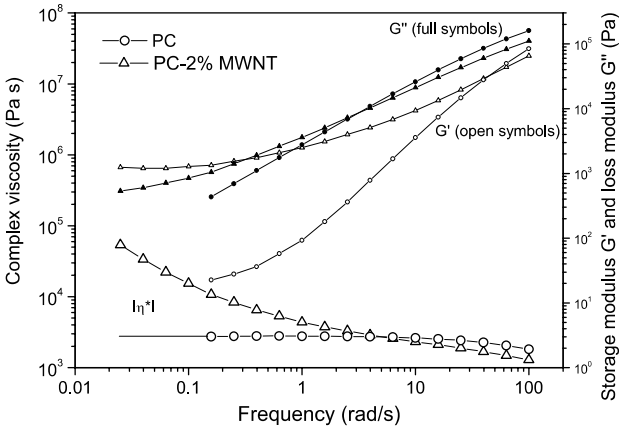

Fig. 2. Melt viscosity $|\eta^*|$, storage modulus G', and loss modulus G'' of PC and PC + 2% MWNT material.

maintaining the SWNT alignment. This procedure was not successful for the PC/MWNT fibers under investigation here.

3. Results and discussion

3.1. Melt spinning behavior

Fig. 2 shows the melt rheological properties of the materials used at 280 °C. The addition of MWNT leads to characteristic changes in the rheological behavior: The complex viscosity shows an increase by decreasing the measurement frequency indicative for the percolated structure of the nanotubes leading to conductivity of the composite. In addition, G' and G'' are increased significantly as compared to pure PC and show a crossover point at a frequency of 0.3 rad/s and G' develops a plateau at low frequencies. At high measurement frequencies, the complex viscosity of the composite is lower than that of the pure PC, which can be related to the additional extrusion step as compared to the initial powder material. Thus, melt spinning behavior of both materials could be different.

Table 2 shows the results of the spinning trials with higher throughput. The spinnability of PC and the composite with 2 wt% MWNT is well, spinning and winding could be done for all experiments without problems, especially there were no fiber breakages. The diameter of the fibers was quite stable as indicated by morphological analysis. Due to the rheological behavior of the material, the estimated melt pressure during the spinning experiments was unusually high in relation to the low throughput and in comparison to other typical melt spinning polymers.

3.2. Alignment of carbon nanotubes along the fiber axis

3.2.1. Morphological analysis

TEM images taken from thin sections prepared along the fiber direction are shown in Fig. 3. It can be seen that this kind of MWNT exhibits a quite curved, spaghetti-like structure, which is far away from the ideal linear structure of MWNT. This is due to defects during the synthesis of the MWNT. As it was shown in a previous paper, in melt-extruded strands of 2 mm diameter no alignment of the same kind of nanotubes was found [17]. Investigations perpendicular and along the axis of the extruded strand did not indicate any preferential orientation. In contrast, the TEM images of the melt spun fibers presented in Fig. 3 clearly show an orientation of the nanotubes in the length axis of the melt spun fibers. With higher draw down ratio the length axis of the MWNT is increasingly oriented with the fiber axis even if they are not completely stretched in the axis. At higher draw down ratios, also a tendency of fiber stretching is observable. The MWNT appear to be more aligned as shown in Fig. 4. This MWNT orientation and alignment cannot be induced or influenced by the cutting procedures since the cut direction which is clearly seen in the images has an angle of 35° to the fiber axis.

3.2.2. Raman spectroscopy

Raman spectroscopy was applied in order to get information of the MWNT orientation, alignment and crystallinity. For interpretation the peak of the G band at 1609 cm^{-1} which is assigned to the in-plane vibrations of the graphitic wall and the peak of the D band at 1284 cm^{-1} originating from disorder in the graphitic structure were used. Parallel to the fiber axis measured Raman spectra are shown in Fig. 5 for the as extruded sample and the fiber with the highest take-up velocity. The intensity ratio D/G is used to assess the degree of crystallinity. A lower ratio indicates a higher crystallinity. The D/G ratios were calculated and compared between the polarization direction parallel and perpendicular to the fiber axis. These D/G ratios are plotted in Fig. 6 in dependence on the draw down ratio indicating that they are more or less independent on the MWNT orientation and alignment. So we can conclude that the crystal structure of the MWNT is not changed through melt spinning.

Interestingly, the D/D and G/G ratios parallel/perpendicular to the fiber axis increases for both bands in a similar manner with the take-up velocity as shown in Fig. 7. This can be explained with an improved alignment/orientation of the MWNT in the fibers through the higher take-up velocity during melt spinning.

3.3. Electrical resistivity of the fibers

The material containing 2 wt% MWNT used for melt spinning shows a volume resistivity of 550 Ω cm, whereas pure PC shows a volume resistivity in the range of 10^{17} Ω cm. However, all the resistance values obtained for the fibers and their bundles were above the measuring range of the Keithley 6517A electrometer, indicating that the fibers are not conductive anymore due to the nanotube orientation and alignment. According to the TEM investigations, this could be easily explained since the probability

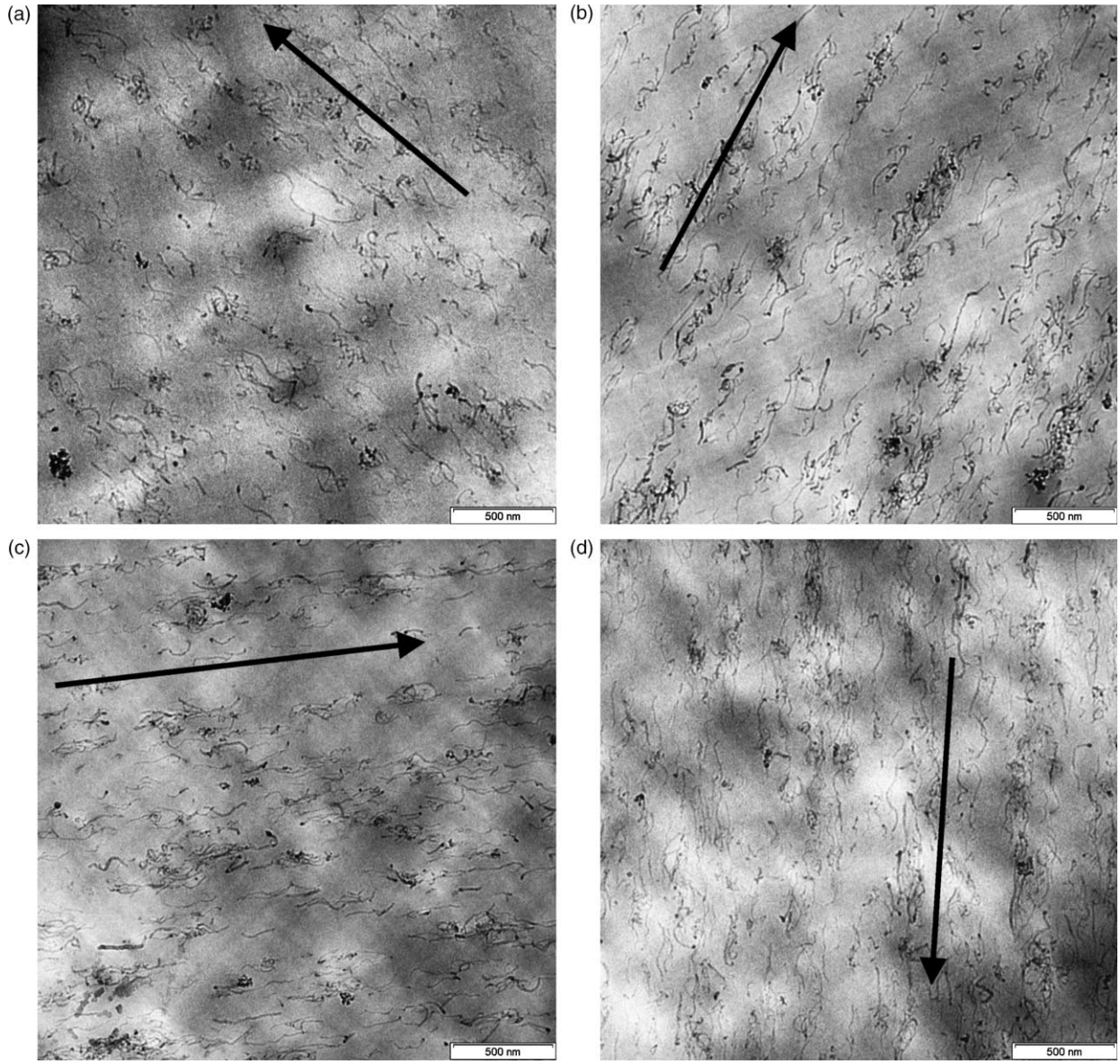

Fig. 3. TEM micrographs of thin sections of the fibers prepared along the fiber axis (assigned by the arrows). In all images the cut direction is 35° to the fiber axis. Varied is the take-up velocity (draw down ratio ddr in brackets): (a) 50 m/min (ddr = 7.8), (b) 200 m/min (ddr = 31.4), (c) 400 m/min (ddr = 62.8), (d) 800 m/min (ddr = 126).

that the MWNT touch each other and form a conducting pathway through the fiber sample is reduced significantly due to the orientation along the fiber. This is in accordance with investigations made by Haggenmueller et al. [6] on melt-processed SWNT/PMMA films which showed high electrical conductivity at low draw ratios but conductivities below the detection limit at draw ratios much higher than four. The authors concluded that the weight fraction of nanotubes necessary for percolation increases as the nanotubes are aligned.

3.4. Mechanical properties of the fibers

The stress–strain behavior of PC fibers as shown in Fig. 8 shows a yield behavior with a cold drawing and strain hardening occurring at higher strains. The stress–strain curves are strongly dependent on the take-up velocity. With increasing draw down ratio resulting in rising fiber tension the orientation of the polymer chains enhances leading to higher stresses. The tensile stress increases significantly and Young's modulus (Fig. 9) increases moderately upon the take-up velocity whereas the elongation at break ε_B (Fig. 10) decreases. This well-known behavior is typical when increasing the fiber take-up velocity.

After adding the MWNT there is qualitative change in the typical stress–strain behavior which again exhibits yielding, cold drawing and strain hardening. At low strains up to the yielding point the nanocomposite fibers shows higher stresses as compared to the PC fibers, leading to higher Young's modulus (Fig. 9). However, the increase in

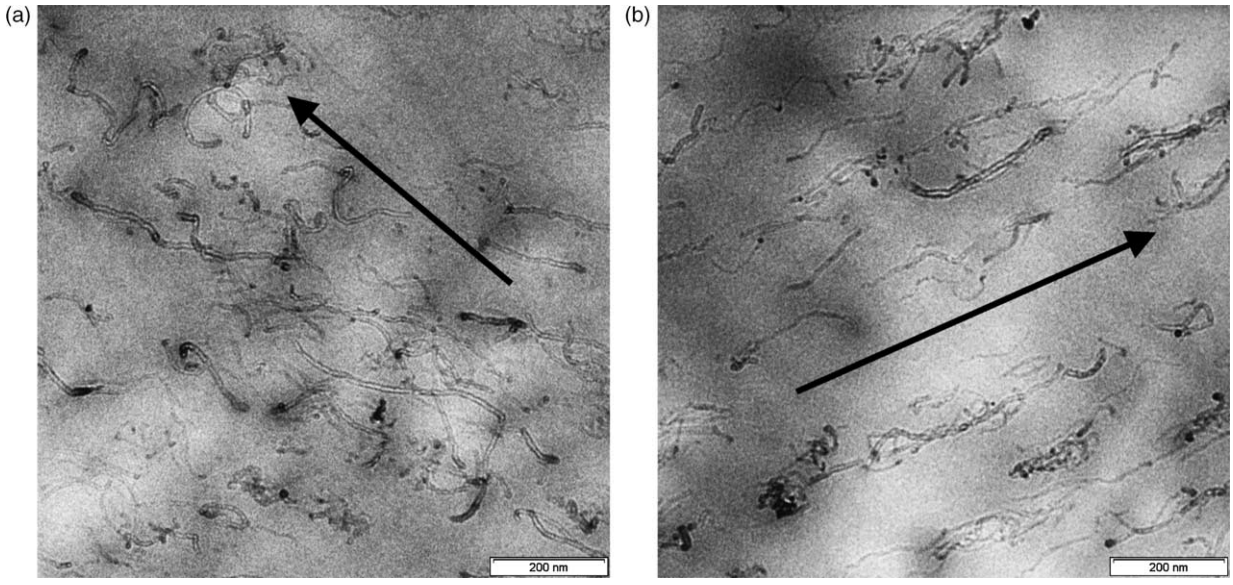

Fig. 4. TEM of thin sections indicating an alignment of the curved MWNT in the fibers. (a) Take-up velocity 50 m/min (ddr=7.8) (b) take-up velocity 400 m/min (ddr=62.8), arrows indicates fiber axis.

Young's modulus is much lower than it could be expected from theoretical calculations. Assuming a modulus of CNT of 500 GPa and a parallel model we should reach as much as 12 GPa for the composite with 2 wt% MWNT. In our case we have to take into account the quite curved structure of the nanotubes leading to some kind of CNT waviness [18], the imperfect adhesion and also the possibility of interwall gliding inside the MWNT as discussed in [19]. All these factors reduce the effective stress transfer leading to much lower increase in modulus than expected. Especially, the CNT waviness was found to influence the effective reinforcing modulus of the nanotubes in a dramatic way as shown by Fisher et al. [18]. Comparing the effective reinforcing modulus of aligned straight CNT with that of wavy CNT in three-dimensional orientation using a combined finite element and micromechanical approach a decrease by a factor of about 10 was found. The experimental values used in this comparison were even lower than these calculations. The increase in modulus described by Sandler et al. [11] on composite fibers of PA12 with entangled catalytically grown MWNT and low draw down ratios is in the same range as found for our composite fibers (about 20% increase). Andrews et al. [20] found an increase in fiber modulus of about 40% at 1.25 vol% addition (about 2.5 wt%) when adding well-aligned high purity MWNT into polypropylene by melt mixing and melt spinning. Bhattacharyya et al. [9] even found a reduction in modulus of PP fibers after addition of 0.8 wt% SWNT. In our composites, the increase in modulus with draw down ratio can be mainly assigned to the higher orientation of the polymer chains and the nanotubes at higher take-up velocities.

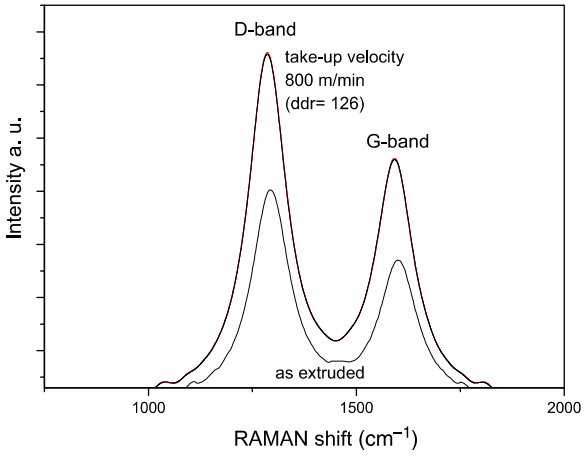

Fig. 5. Raman spectra taken parallel to the fiber axis for as extruded fiber and take-up velocity of 800 m/min (ddr=126) indicating the *D* band at 1284 cm^{-1} and the *G* band at 1609 cm^{-1}.

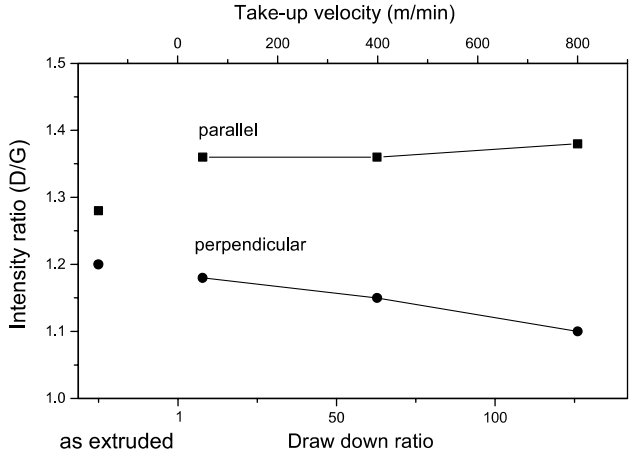

Fig. 6. Raman spectroscopy: Intensity ratios of the *D* and *G* bands in both polarization directions parallel and perpendicular to the fiber axis.

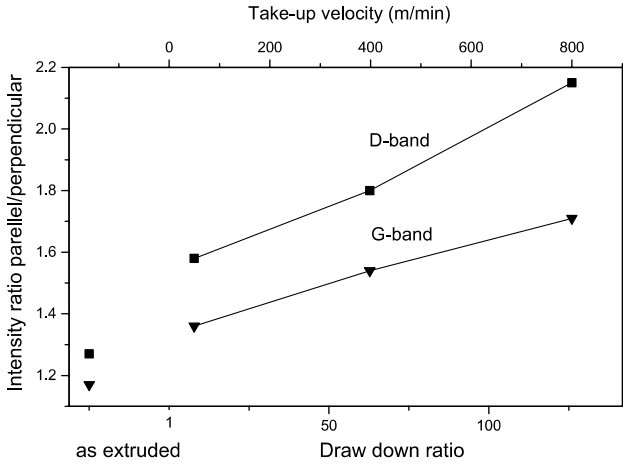

Fig. 7. Raman spectroscopy: Intensity ratios parallel/perpendicular to the fiber axis of the *D* band and *G* band.

After the yield point the stresses at a given strain are lower in the nanocomposites than in the PC fibers resulting in lower stresses at break. The nanotubes seems to act as imperfections what often is observed for composites exhibiting cold drawing/strain hardening beyond the yield point. Again the elongation at break decreases with the draw down ratio, however, in a lower extent as compared to the PC fibers (Fig. 10) leading finally at the draw down ratio of 126 to a value higher than that of PC.

Regarding the tensile stress at break the different fiber diameters by changing the draw down ratio have to be taken into account. Increasing draw down ratio leading to higher polymer chain orientation results in higher tenacity, which is the breaking force F_B with respect to initial cross-section A_0 of the fiber. In order to reflect the dependencies in a proper manner, the true stress at break σ_B, which is the force at break related to the actual fiber cross-section at break is calculated using

$$\sigma_B = \frac{F_B}{A_0}\left(1 + \frac{\varepsilon_B}{100\%}\right)$$

This value is normally nearly independent on the process history for common melt spinning polymers. The true stress

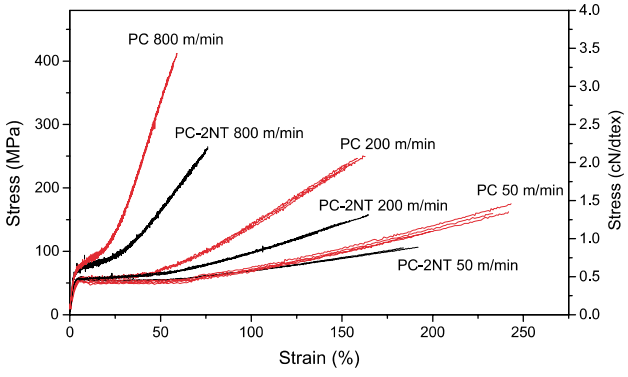

Fig. 8. Stress–strain behavior of the fibers (three measurements are plotted for each sample).

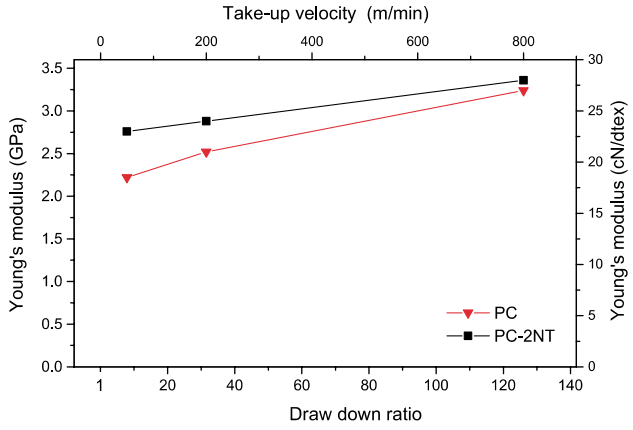

Fig. 9. Young's modulus (at 1% strain) vs. draw down ratio.

at break of pure PC lies between 480 and 540 MPa (4–4.5 cN/dtex) as shown in Fig. 11 and does not change significantly with the draw down ratio. A quite different elongational behavior was observed for the MWNT filled fibers. At low draw down ratio, i.e. at low orientation, the true stress at break is lower than for the PC fibers, which results as well from the lower stress at break as the lower elongation at break. However, with increasing the draw down ratio the true stress at break increases and reaches a comparable value at the highest draw down ratio.

The finding of a reduced elongation at break after adding nanofillers is in accordance to observations by Sandler et al. [11] on fibers of PA12 with MWNT and carbon nanofibers prepared under constant draw ratio by varying the amount of nanofiller. Also, Siochi et al. [7] found a significant decrease in elongation at break in their SWNT/polyimide fibers. In our investigations, however, with increasing draw down ratio and increased orientation the composite with 2 wt% MWNT leads to higher values of elongation at break than the pure PC. It seems that for higher orientation the drawability of the 2 wt% MWNT filled material becomes better than for the unfilled one. The better drawability correlates indeed with the (true) stress vs. draw down ratio

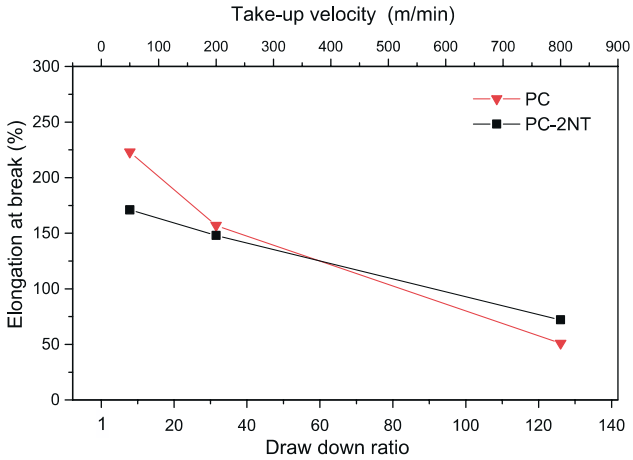

Fig. 10. Elongation at break vs. draw down ratio.

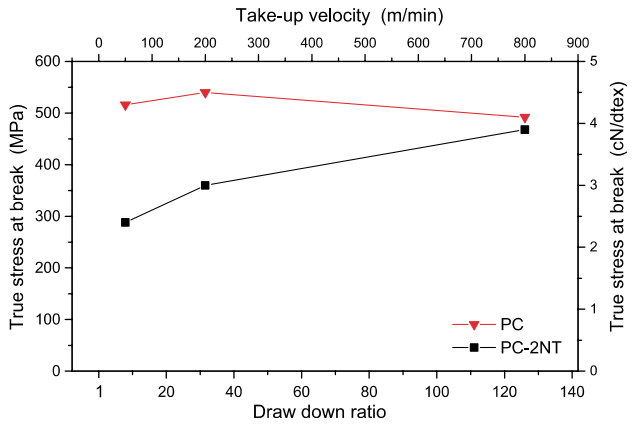

Fig. 11. True stress at break vs. draw down ratio.

behavior which was shown to increase with the spinning orientation.

4. Summary and conclusions

Composites of polycarbonate with 2 wt% multiwalled carbon nanotubes and the corresponding pure PC were melt spun using a piston type spinning device. Different take-up velocities up to 800 m/min and throughputs were used. For composites prepared at a constant throughput of 0.45 cm^3/min an orientation of the nanotubes length axis along the fiber axis was shown using TEM investigations. The nanotubes align in their length axis along the fiber axis increasingly with the draw down ratio varied up to 126, however, the curved shape of the nanotubes still exist in the melt spun fibers. Finally, at higher draw down ratio the MWNT started to align by reducing their curvature. Polarized Raman spectroscopy indicated that the *D*/*D* and *G*/*G* ratios parallel/perpendicular to the fiber axis increase for both MWNT bands in a similar manner with the draw down ratio. Interestingly, with increasing alignment electrical conductivity of the fibers is lost. Mechanical properties of the composites were tested and compared using the stress–strain behavior of the fibers. Young's modulus shows an increase of about 24% at low draw down ratio after addition of 2 wt% MWNT composite which lowers with higher draw down ratio. This relatively low increase can be assigned mainly to the high waviness of the MWNT material. At low spinning speeds, elongation at break and tensile strength of the composites with 2 wt% MWNT are lower than those of the pure PC. However, the increase of true stress at break with the draw down ratio is higher and the decrease of elongation at break with draw down ratio is lower in case of the composites as compared to PC. Therefore, at the high draw down ratio of 126, elongation at break is higher and stress at break is comparable to the melt spun PC fibers. This could be connected to the loss of the percolated structure of the MWNT with increasing alignment so that the polymer chains can have a higher mobility than in the restricted structure within the percolated nanotube network and the reinforcing effect of the nanotubes becomes more effective.

Acknowledgements

We thank Dr Brzezinka (BAM Berlin) for performing the RAMAN measurements and Dr Goering for help by their quantification.

References

[1] Marcinčin A. Prog Polym Sci 2002;27(5):853–913.
[2] Dalton AB, Collins S, Razal J, Munoz E, Ebron VH, Kim BG, et al. J Mater Chem 2004;14(1):1–3.
[3] Abdelkader M, Withers JC, Loutfy RO, Moravsky A, Sennett M. 23rd Army science conference 2002.
[4] Kumar S, Dang TD, Arnold FE, Bhattacharyya AR, Min BG, Zhang XF, et al. Macromolecules 2002;35(24):9039–43.
[5] Kearns JC, Shambaugh RL. J Appl Polym Sci 2002;86(8):2079–84.
[6] Haggenmueller R, Gommans HH, Rinzler AG, Fischer JE, Winey KI. Chem Phys Lett 2000;330(3–4):219–25.
[7] Siochi EJ, Working DC, Park C, Lillehei PT, Rouse JH, Topping CC, et al. Composites B 2004;35:439–46.
[8] Haggenmueller R, Zhou W, Fischer JE, Winey KI. J Nanosci Nanotechnol 2003;3:105–10.
[9] Bhattacharyya AR, Sreekumar TV, Liu T, Kumar S, Ericson LM, Hauge RH, et al. Polymer 2003;44:2373–7.
[10] Sennett M, Welsh E, Wright JB, Li WZ, Wen JG, Ren ZF. Appl Phys A-Mat Sci Process 2003;76(1):111–3.
[11] Sandler JKW, Pegel S, Cadek M, Gojny F, Van Es M, Lohmar J, et al. Polymer 2004;45(6):2001–15.
[12] Sreekumar VT, Liu T, Min BG, Guo H, Kumar S, Hauge RH, et al. Adv Mater 2004;16(1):58–60.
[13] Lucas M, Vigolo B, Badaire S, Le Bolloc'h D, Marucci A, Durand D, et al. AIP Conf Proc 2002;633:579–82.
[14] Zhou W, Winey KI, Fischer JE. Mater Res Soc Symp Proc 2003;740: I12.21.1.
[15] Du F, Fischer JE, Winey KI. J Polym Sci, Part B: Polym Phys 2003; 41:3333–8.
[16] Pötschke P, Fornes TD, Paul DR. Polymer 2002;43(11):3247–55.
[17] Pötschke P, Bhattacharyya AR, Janke A. Eur Polym J 2004;40(1): 137–48.
[18] Fisher FT, Bradshaw RD, Brinson LC. Appl Phys Lett 2002;80(24): 4647–9.
[19] Gojny FH, Nastalczyk J, Roslaniec Z, Schulte K. Chem Phys Lett 2003;370:820–4.
[20] Andres R, Jacques D, Rantell T. Macromol Mater Eng 2002;287: 395–403.